Engineering Journal issn: 0125-8281

Article

Effects of Carbonation on Corrosion Rate of Reinforcing Steel in Different Concrete and Repair Materials

Sothyrak Rath[1,a], Pakawat Sancharoen[2,b,*], Pitichon Klomjit[3], and Somnuk Tangtermsirikul[1]

1 School of Civil Engineering and Technology, Sirindhorn International Institute of Technology, Thammasat University, Thailand
2 Construction and Maintenance Technology Research Center, Sirindhorn International Institute of Technology, Thammasat University, Thailand
3 National Metal and Materials Technology Center, Thailand
E-mail: [a]rathsothyrak2222@gmail.com, [b,*]pakawat@siit.tu.ac.th (Corresponding author)

Abstract. Reinforced concrete with different concrete mix proportions, i.e. binder types or w/b ratio, would provide different quality to protect the reinforcing steel from corrosion. When carbonation occurred, corrosion of steel embedded in concrete can be initiated. This paper reports effects of carbonation on electrochemical properties of steel embedded in concrete with different mix proportions as w/b ratio of 0.4 and 0.6, fly ash added up to 30% by weight of binder, and also in six repair materials. All samples was exposed to accelerated carbonation (4% CO_2, 50 ± 5% relative humidity (RH), and 40 ^{0}C temperature) and laboratory environment (0.04% CO_2, 75 ± 5% RH, and 28 ^{0}C). The electrical resistivity was monitored by using four-point Wenner probe. The Linear polarization resistance (LPR) was used to characterize the corrosion rate of embedded steel at different exposure time. The carbonation depth of specimens was also tested by using the phenolphthalein indicator. The void contents of repair material specimens were also determined. The results showed that the electrical resistivity of concretes and repair materials increased along with an increase of carbonation depth. However, in case of fly ash concrete, the electrical resistivity decreased at longer exposure period in accelerated carbonation due to decomposition of C-S-H by carbonation. It was also found that the corrosion rate of steel embedded in concrete and repair materials increased as an increase of carbonation depth, even the carbonation depth was less than the covering depth. Steel embedded in ordinary Portland cement (OPC) concrete or low w/b concrete shows lower corrosion rate due to higher pH of concrete. The guideline for evaluation of corrosion initiation and severity due to carbonation is also proposed.

Keywords: Corrosion, patching, grouting, carbonation, electrical resistivity, electrochemical, polarization resistance.

ENGINEERING JOURNAL Volume 25 Issue 6
Received 27 October 2020
Accepted 5 June 2021
Published 30 June 2021
Online at https://engj.org/
DOI:10.4186/ej.2021.25.6.75

DOI:10.4186/ej.2021.25.6.75

1. Introduction

Nowadays, many reinforced concrete structures have been exposed to aggressive environments that could cause premature deterioration of structures. Among those causes, corrosion has been considered as a major problem that leads to reduction of service life of structures, especially for those have been exposed to chloride or carbonation environments [1].

In reinforced concrete structures, the embedded steel is normally protected from corrosion by chemical and physical protection from its surrounding concrete [2]. Physical protection consists of the quality of surrounding concrete to withstand the ingress of harmful species as well as the permeability of water. Whereas, the chemical protection is formed by the presence of alkalinity in concrete pore solutions that generates high pH value to ensure the stability of the passive film, (FeO or Fe_2O_3), which forms around steel surface. Under carbonation, the CO_2 from environment dissolves in concrete pore solutions forming carbonic acid. The carbonic acid reacts with the alkaline in concrete, mainly CH and C-S-H, forming calcium carbonate. As a consequence of this reaction, the pH in pore solutions is considerably reduced that leads to weakening the chemical barrier. This reduction of pH leads to an instability of the passive film that could cause the corrosion initiation.

In general, the carbonation of concrete structures with OPC-cement based is considered as a slow process due to their sufficient amount of CH availability to react with CO_2 [3]. Additionally, this slow process attributes to an enhancement of concrete properties such as a decrease of permeability and an increase of surface hardness due to the deposition of carbonates in the pore microstructure [2, 4]. The introduction of supplementary cementitious materials (SCMs) has been increasingly earned interest in civil engineering application due to their ability to reduce the environmental footprints such as the reduction of CO_2 emission as well as the re-use of certain waste and by-product materials. Regarding to this, many studies [5-10] has been focused on their resistance against carbonation since all of these SCMs have lower amount of generated CH than that of OPC concrete. Some studies proposed that the addition of SCMs can reduce the carbonation rate due to reduction of concrete permeability and CO_2 penetration rate [11]. However, some other studies revealed that the addition of SCMs leads to faster carbonation rate as well as influencing carbonation of concrete properties [10, 12]. Papadakis [13] found that the substitution of SCMs in concrete could lead to both positive and negative effects on carbonation resistance. He found that the carbonation rate increased when the SCMs were substituted for cement and the effect was inverse when the SCMs were used as aggregates replacement in concrete mix proportions. Auroy et al. [14] found that the carbonation leads to a decrease of permeability in OPC concrete, which is in contrast to the carbonation of blended cement concrete that the permeability increased. This increase of permeability of blended cements concrete attributed to the micro-cracking from the effect of carbonated C-S-H [7].

Al-Zahrani et al. [15] studied effect of carbonation on polymer-based and cement-based repair materials. The results showed that there was a large variation of durability in each types of repair materials that attributed to the difference in their composition. They also found that most of polymer-based repair mortars revealed higher electrical resistivity than those of cement-based repair mortars. However, the results of carbonation depth of polymer-based repair mortars revealed a contradict phenomenon, which polymer-based mortars showed higher depth of carbonation than those of the cement-based mortars. This attributed to the types and amount of polymer used in these polymer-modified mortars that favoring the carbonation reaction.

Regarding to electrochemical properties of steel in carbonation-induced corrosion, Glass et al. [16] found that there was no significant corrosion observed before carbonation depth reached the steel. In contrast, the corrosion rate increased when the remaining uncarbonated length ranged from 5 mm to -10 mm [17]. This attributed to endangerment of the passive film by carbonation. Chavez et al. [18] found that the corrosion was not occurred at the low relative humidity, even the carbonation front already reached the steel. This attributed to the lack of moisture supply for the corrosion reaction at the cathodic region. Serdar et al. [3] found that the corrosion rate of steel embedded in OPC mortar was still low, even the carbonation already reached the steel; unlike the case of steel embedded in low alkalinity mortar. This attributed the passive film of steel in OPC mortar was not completely destroyed when the carbonation front reached the steel surface, while it was completely destroyed in case of low alkalinity mortar.

A large variation has been observed on the carbonation properties and electrochemical properties of steel in different types of concretes. The effects of carbonation and types of binders on electrochemical behavior of steel still remain uncertain. The application of fly ash as cement replacement in Thailand has grown interest due to the availability of material as well as the aim of reduction of environmental footprint. However, the effect of carbonation on corrosion behavior of steel embedded in this blended fly ash concrete still remains unknown. In addition, when the corrosion occurred, the repair of that corroded zone is needed. Hence, the study of the corrosion behavior of steel in those repair materials is needed in order to select a suitable materials.

The aim of this paper is to study about the effect of carbonation on the corrosion behavior of steel embedded in OPC concrete together with OPC blended fly ash concrete with different w/b ratio. In addition, the steel embedded in selected repair materials that are presently used for repairing the deteriorated reinforced concrete structures were also presented in this study. The phenolphthalein indicator, Four-point Wenner probe, Linear polarization resistance (LPR), and Electrochemical

impedance spectroscopy (EIS) were conducted in this study.

1.1. Significance of study

From this study, the electrochemical properties of reinforcing steel embedded in concrete and repair materials corroded by carbonation can be understood. Evaluation of corrosion initiation based on carbonation depth can be more accurate. Service life evaluation and prediction of reinforcing steel corrosion due to carbonation can be proposed. The selections of repair materials for carbonated reinforced concrete can be recommended.

2. Experimental program

2.1. Materials

Four types of concrete mixes with the variation of w/b ratios 0.4 and 0.6, as well as the fly ash replacement 0 and 30% by weight of binder were used. The cement used was type-I OPC that conformed to ASTM C150 [19]. The fly ash was type-2b coal fly ash conformed to TIS2135 [20]. The river sand, with specific gravity of 2.67, and crushed limestone, maximum size of 10 mm and specific gravity of 2.85, were prepared for concrete mixes. The amount of aggregates were the same and fixed in all mix proportions. The summary of concrete mix proportions is shown in Table 1.

The steel bars being used were deformed reinforcing steel with diameter of 12 mm and grade SD40 according to TIS 24-2548(2005).

Six different brands of repair materials that are widely used for repairing the deteriorated reinforced concrete structures were selected. Three of the selected repair materials were polymer or fiber-modified cementitious patching materials, while the others were cementitious grouting materials. Table 2 and 3 summarizes details and compositions of the repair materials used in this study.

2.2. Specimen preparation and exposure conditions

The steel bars with 150 mm length were coated with epoxy leaving only 60 mm length which is 22.608 cm^2 surface area to be uncoated and being exposed inside the concretes and repair materials. Figure 1 shows the details of the preparation of steel bar.

Three shapes of samples were prepared according to different tests. The cubic 150 × 150 × 150 mm, was prepared for electrical resistivity test as shown in Fig. 2(a).

Table 1. Mix proportions of concrete.

Name	w/b	Fly ash (%)	Unit Content (kg/m^3)				
			Cement	Fly Ash	Water	Gravel	Sand
0.4OPC	0.4	0	396.8	0	158.7	1103.4	805.9
0.4FA	0.4	30	261.5	112.1	149.4	1103.4	805.9
0.6OPC	0.6	0	314.5	0	188.7	1103.4	805.9
0.6FA	0.6	30	210.1	90.1	180.1	1103.4	805.9

Table 2. Details of repair materials.

Repair materials	Description	Mix proportion (w/p)	Layer thickness (mm)	Compressive Strength (MPa)
PSK	Pre-packed blend of sulphate resistant cement, selected aggregates and additives	0.155	50	50
PSB	Pre-packed blend of cement, polymer, special fiber	0.18	40	54.4
PLK	Pre-packed blend of cement, hydraulic binder, mineral filter and specific additives	0.18	50	60
GSK	Pre-packed of cementitious grout	0.16	50	54
GSC	Pre-packed of cementitious grout	0.18	-	-
GPU	Pre-packed blend of lime based expansive additive, fine aggregate, cement and special admixtures	0.148	-	67.5

Table 3. Material composition of repair materials.

Repair materials	Material compositions						
	Cement	Polymer	Fiber	Aggregates	Sand	Additives	Admixures
PSK	√		√	√		√	
PSB	√	√	√				
PLK	√		√		√		√
GSK	√					√	
GSC	√					√	
GPU	√			√		√	

DOI:10.4186/ej.2021.25.6.75

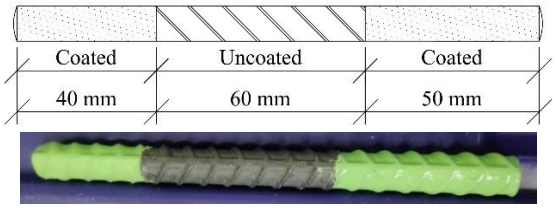

Fig. 1. Preparation of steel bars.

This dimension was selected following the criteria of Gower and Millard [21]. The long prismatic samples were prepared for carbonation depth test with the dimension of 240 × 100 × 60 mm and 240 × 100 × 40 mm for concretes and repair materials, as shown in Fig. 2(b) & (c), respectively. The reinforced concrete and repair material samples were prepared by embedded steel bars, as shown in Fig. 1, inside prismatic samples 100 × 100 × 60 mm and 100 × 100 × 40 mm for concrete and repair materials, as shown in Fig. 2(d) & (e), respectively. The covering depth in case of concrete samples was 20 mm while it was only 10 mm in case of repair materials. Smaller covering depth for repair materials was chosen due to the time limit in this study since repair materials were expected to have higher resistance to carbonation than that of concrete.

For the void content test for repair materials, the triplicate samples of 50 × 50 × 50 mm were prepared and performing the test at the age of 28 days after plastic-wrap curing condition. The test was performed according to ASTM C642 [22].

The concrete and repair material samples were demolded one day after casting and then were cured with plastic wrap for 28 days. After the curing period, all samples were exposed to a normal room environment, with 75 ± 5 % relative humidity (RH) and 28 ^{0}C Temperature (T), for 30 days in order to reduce their initial moisture content that could affect to early carbonation exposure.

All concrete and repair material samples were coated their surface with epoxy painting leaving only one face being exposed to carbonation exposures.

For electrochemical test and carbonation depth test samples, the uncoated surface was the top casting surface, while the side face was uncoated for electrical resistivity test samples. Figure 3 shows the coated and uncoated surface of samples.

Each types of samples were divided into two groups for two exposure conditions. One group was exposed to normal laboratory environment (0.04% CO_2, 75 ± 5 % RH, and 28 ^{0}C T) named as, for concrete: 0.4OPCL, 0.4FAL, 0.6OPCL and 0.6FAL, for patch-repair materials: PSKL, PSBL, and PLKL, and for grout-repair materials: GSKL, GSCL and GPUL. Another group were exposed to accelerated carbonation environment (4% CO_2, 50 ± 5% RH, and 40 ^{0}C T) named as, for concrete: 0.4OPCA, 0.4FAA, 0.6OPCA and 0.6FAA, for patch-repair materials: PSKA, PSBA, and PLKA, and for grout-repair materials: GSKA, GSCA and GPUA. The samples were being exposed until the carbonation depth reached the steel surface and corrosion was initiated.

For corrosion and electrical resistivity monitoring, the samples were conditioned inside a high humidity box for one day before test, called Dry state. This preconditioning of samples before testing was applied to all samples at the testing time of 0, 10 and 27 days of exposure period. Another approach of preconditioning of samples, called Moist state, was conducted by wetting the samples for 30 minute and kept in a humidity box for one day before test. This approach was applied at the exposure period longer than 45 days onwards because sample is too dry for measuring.

2.3. Test procedures

Four types of tests were performed in this study as phenolphthalein indicator for carbonation depth, four-point Wenner probe for electrical resistivity test, Linear polarization resistance (LPR) for corrosion monitoring and electrochemical impedance spectroscopy (EIS) for electrical resistance of concretes and repair materials.

The carbonation depth were performed with the samples shown in Fig. 2(b) & (c). These long samples were dry grooved at distance about 50 mm from the end.

This grooved sample was then split, brushed and sprayed with phenolphthalein. The colorless region after spraying phenolphthalein was considered as carbonated

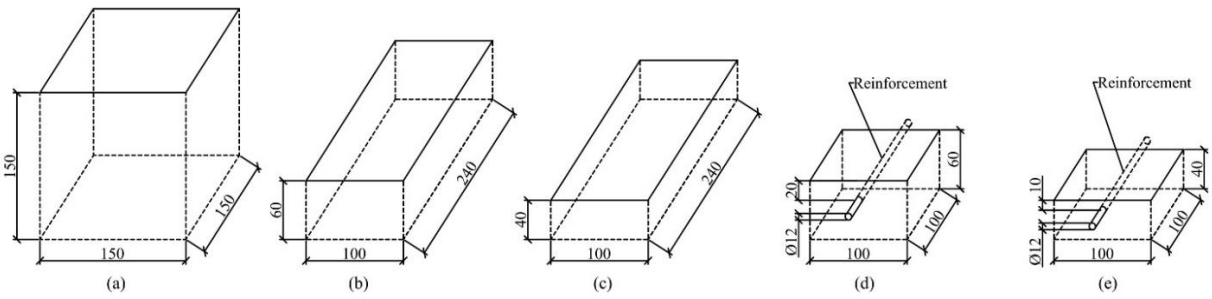

Fig. 2. Types and dimensions of samples: (a) electrical resistivity for both, concretes and repair materials; (b) carbonation depth for concretes; (c) carbonation depth for repair materials; (d) electrochemical for concretes; and (e) electrochemical for repair materials.

region and the purple region referred to noncarbonated region. The result of the carbonation depth was the average of five measuring points of the split surface.

The electrical resistivity was performed by using four-point Wenner probe test method. The Resispod Resistivity Meter equipment with probe spacing of 38 mm was used in this test. The test was conducted by wetting the tips of the four electrodes with water and then placing them on the uncoated surface of sample. The measured electrical resistivity values were the average of four measurements at the middle, orthogonal to width and length of exposed surface, as shown in Fig. 4.

The corrosion monitoring was done by Linear polarization resistance (LPR) measurement. The test was performed by using Metrohm PGSTAT302N. The three-electrode system, as shown in Fig. 5, with working electrode (WE) was embedded steel bar, the counter electrode (CE) was stainless steel plate that was placed on the exposed surface and being connected to concrete/repair material surface by conductivity gel, and the reference electrode (RE) was saturated copper/copper sulfate (CSE) reference electrode that was placed on the center of exposed surface area.

Before starting the LPR measurement, the waiting time of 5 minutes for stabilizing open circuit potential (OCP) was used. The LPR measurement was performed by polarizing the steel ±10 mV from measured open circuit potential (OCP) with the scan rate of 0.5 mV/s. The ohmic drop effect from the concrete/repair material resistance was also taken into account by subtracting the cover resistance from measured polarization resistance.

The corrosion current from LPR was calculate by using Stern-Geary [23] equation as shown in Eq. (1):

$$I_{corr}=B/R_p \quad (1)$$

where I_{corr} is corrosion current (μA),
R_p is polarization resistance after compensating ohmic drop (kΩ),
and B is a constant and equals to 26 mV [24].

Then this corrosion current was converted to corrosion rate (CR) in mg/cm²-year by Eq. (2) [25]. The corrosion severity can be classified as shown in Table 4 [26].

$$CR=3.65\times K_2\times \frac{I_{corr}}{A}\times EW \quad (2)$$

where CR is corrosion rate of the steel (mg/cm²-year),
K_2 is a constant and equals to 0.08954 g-cm²/μA-m² day,
A is an exposed surface area and equals to 22.608 cm².
EW is a dimensionless equivalent weight which equals to 27.92 for Fe with valence 2.

The electrical resistance of covering concrete and repair materials were monitored by performing the Electrochemical Impedance Spectroscopy (EIS). The EIS was monitored by applying the AC perturbation of ±10 mV from OCP with frequency range between 10^5 Hz and 10^{-2} Hz. The fitting data was carried out using Nova 1.11 software with the equivalent circuit as shown in Fig. 6. The couple CPE-R_c that performed at high frequency, referred to dielectric properties of concrete that consists of concrete resistance (R_c). The CPE_P-R_P couple, at low frequency range, characterizes corrosion process of steel/concrete interface that R_P is polarization resistance of reinforcing steel. The Rs is solution resistance.

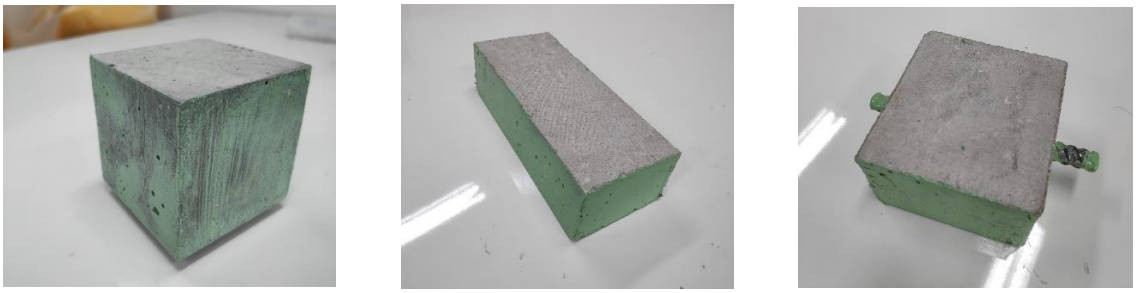

Fig. 3. Specimens with coated side-surfaces and uncoated top-surface for: (a) electrical resistivity test; (b) carbonation depth test; and (c) electrochemical test.

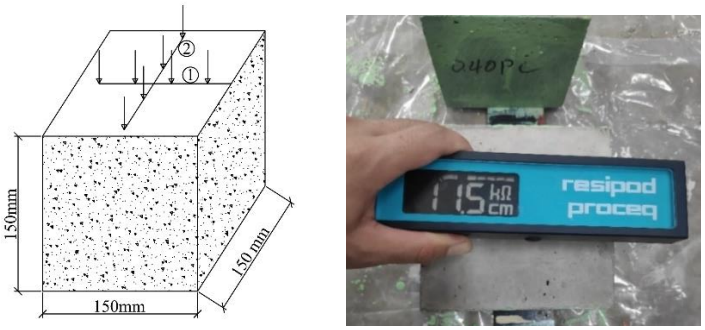

Fig. 4. Set-up and positions of electrical resistivity measurement. Point 1 and 2 are the positions where the tips of equipment were placed.

DOI:10.4186/ej.2021.25.6.75

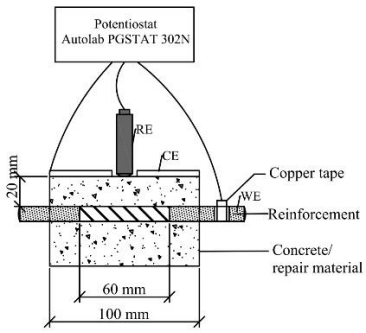

Fig. 5. Set-up of LPR and EIS measurement.

Table 4. Characterization of corrosion probability [26].

Severity level	Corrosion rate (mg/cm^2-yr)
Passivity	< 0.91
Low corrosion	0.91 - 4.55
High corrosion	4.55 - 9.10
Extremely high corrosion	> 9.10

All of the tests were performed at 0, 10, 27, 60, 120, and 150 days after being exposed to carbonation.

It should be noted that the tests of 0.6FA, and 0.6OPC were finished at the exposure period of 117, and 135 days, respectively, because corrosion was initiated. All test was conducted on duplicate samples and average results are reported.

3. Results and discussion

3.1. Carbonation depth

Figures 7 and 8 show experimental results of carbonation depth versus square root time of concrete and repair materials, respectively.

The effect of fly ash replacement in concrete on carbonation depth was observed in Fig. 7. The carbonation rate of fly ash concrete is higher than OPC concrete. This result is in good agreement with the previous researches [10, 12, 14]. This is because reduction of $Ca(OH)_2$ content in FA concrete [3] leads to faster rate of carbonation.

In addition, the effect of w/b ratio on carbonation rate was also observed in Fig. 7, which is similar to results of other researches [27, 28]. The carbonation rate of higher w/b concrete was higher than the lower w/b concrete. This is because high w/b ratio concrete has higher porosity.

The carbonation rate of repair materials were lower than concrete. Only PSKA and PSBA that showed progress of carbonation which is comparable 0.4OPCA, as shown in Fig. 8. Superior carbonation resistance of repair materials is due to void content of repair materials is lower than that of concrete, as shown in Table 5. This can be due to additives i.e. expansive agent or polymer, larger cement content and good gradation of materials.

3.2. Electrical resistivity

Figures 9, 10 and 11 show experimental results of electrical resistivity measured by Wenner probe method of concrete, patch repair and grout repair materials, respectively. The electrical resistivity decreased as an increase of w/b ratio for each types of concretes (FA and OPC concrete), as shown in Fig. 9. This result is in good agreement with other studies [27, 29].

Moreover, electrical resistivity of concrete specimens increased along with an increase of exposure period, as shown in Fig. 9, which is in good agreement with other studies [30, 31]. This attributes to hydration reaction of cement that reduces interconnected pores networks of concrete. In addition, for FA concrete, this increase of resistivity attributed to the formation of C-S-H gel from the pozzolanic reaction that further refines the concrete pores [32-34].

Specimens that were exposed to accelerated carbonation showed an increasing of electrical resistivity, as shown in Fig. 9. This is due to deposition of $CaCO_3$ that clogged capillary pore [4]. However, for 0.4OPCA, 0.4FAA and 0.6FAA samples, the electrical resistivity decreased at the end of the graph. This attributed to the insufficiency of CH to reacts with CO_2, as a result, other hydration products started to react with CO_2, especially C-S-H [8, 14]. The carbonation of C-S-H leads to the creation of poorly crystalline or even amorphous $CaCO_3$ that could be the reason that this product of carbonation does not create the same pore clogging effect mention earlier. Another reason, this was attributed to the decomposition of C-S-H, forming silica gel and micro-cracking. It should be noted that this mechanism can be observed only in accelerated carbonation, which has high CO_2 concentration. This phenomenon may not occur in natural carbonation due to the low CO_2 concentration in environment.

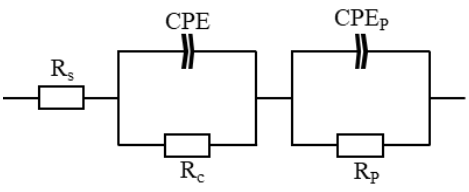

Fig. 6. Equivalent circuit used to fit the impedance spectra.

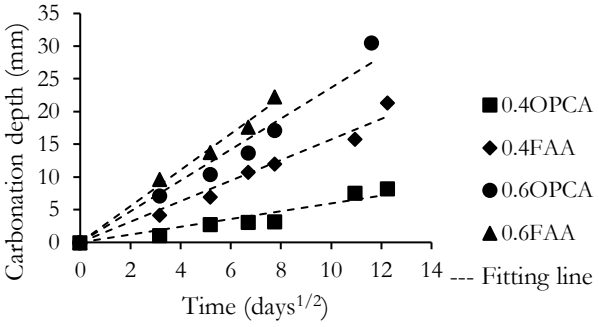

Fig. 7. Carbonation depth versus square root of time of concretes being exposed to accelerated carbonation.

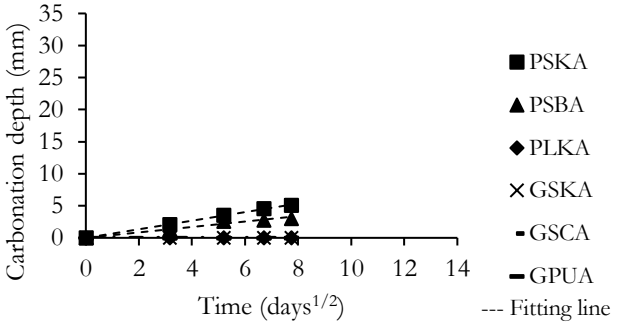

Fig. 8. Carbonation depth versus square root of time of repair materials being exposed to accelerated carbonation.

Electrical resistivity of patch repair is comparable to concrete, as shown in Fig. 10. Only the electrical resistivity of PSKA and PSBA significantly increased with exposure period in accelerated carbonation. This is due to progress of carbonation of these two materials as previously explained.

It should be noted that even void content of PSB was the highest, as shown in Table 5, but its electrical resistivity showed the highest value among all repair materials due to there is a polymer mixed in the composition of PSB as shown in Table 3.

The electrical resistivity of grout materials also shows similar value to 0.4OPC, as shown in Fig. 11. Since there was no carbonation on these materials, thus no significant change of electrical resistivity was observed.

Table 5. Void content of repair materials and concrete at the age of 28 days after curing.

Samples	Void content (%)	Reference
PSK	9.12	
PSB	9.43	
PLK	8.49	
GSK	8.13	
GSC	6.66	
GPU	8.77	
Concrete samples		
0.4OPC	16.1	[35]
0.6OPC	20.18	[36]

3.2.1. Comparison of electrical resistance measured by EIS and Wenner probe

The comparisons of the electrical resistance of 0.4OPC specimen measured by Wenner probe, denoted $R_{c,Wenner}$, and electrical resistance measured by EIS, denoted $R_{c,EIS}$, is shown in Fig. 12. The results show the same tendency but Wenner probe shows lower electrical resistance than EIS. This is because EIS measures resistance of concrete only the region from the steel surface to the exposed surface (covering concrete). While Wenner probe measures around 5 to 10 cm [37] from the exposed surface as shown in Fig. 13. The covering concrete is normally drier than at the deeper depth. Therefore, resistance measured by EIS is higher than Wenner probe. Moreover, significant difference of concrete resistance is observed in the samples exposed to accelerated carbonation. This is because carbonation affects electrical resistivity of concrete measured by both of Wenner's probe and EIS, as shown in Fig. 12 and 13. Due to pore densification by carbonation product as calcium carbonate [4], resistivity increased. However, EIS measures mainly concrete properties between working electrode and counter electrode which are embedded reinforcing steel and stainless steel on concrete surface, respectively. While Wenner's probe measure concrete properties up to 5 to 10 cm of concrete depth [37]. As a result, effect of carbonation on increasing of electrical resistivity is clearly observed in case of EIS.

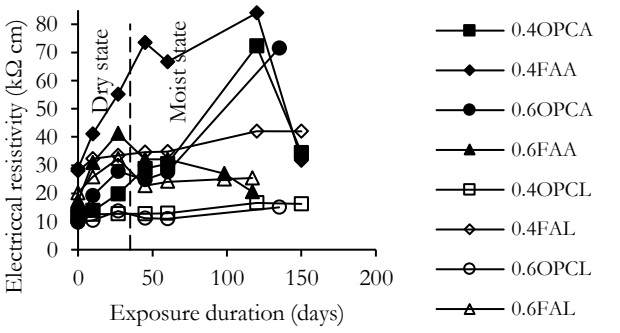

Fig. 9. Electrical resistivity versus exposure duration of concretes being exposed to accelerated carbonation and laboratory environment.

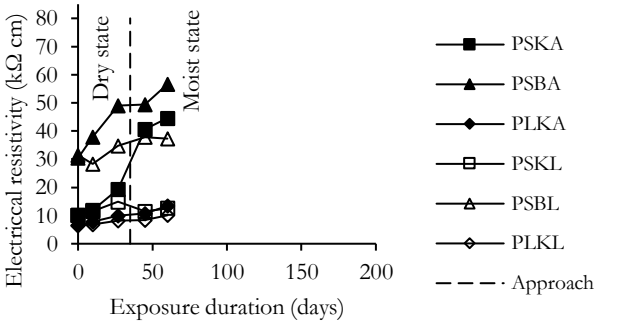

Fig. 10. Electrical resistivity versus exposure duration of patch-repair materials being exposed to accelerated carbonation and laboratory environment.

DOI:10.4186/ej.2021.25.6.75

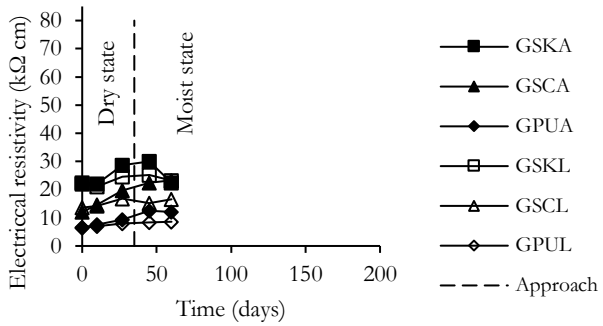

Fig. 11. Electrical resistivity versus exposure duration of grout-repair materials being exposed to accelerated carbonation and laboratory environment.

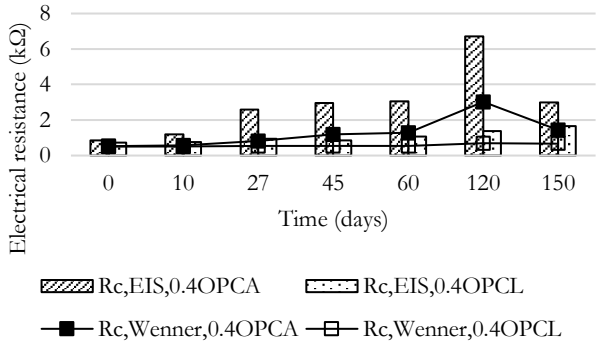

Fig. 12. Comparison of electrical resistance measured by EIS and Wenner probe of the 0.4OPC specimen.

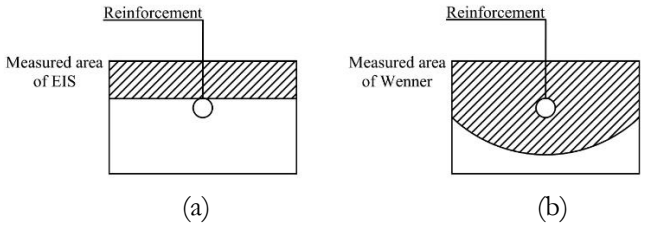

Fig. 13. Electrical resistance measured from: (a) EIS, and (b) Wenner probe.

3.3. Corrosion rate

The relationship between corrosion rate and mass loss are discussed in Topic 2.3. Corrosion rate can be expressed in different ways as, corrosion current density (μA/cm²), as section loss rate of the steel section diameter (mm/year) or as mass loss rate (CR) (mg/cm² year). The relationship between mass loss and corrosion current density can be expressed through Faraday's law, as shown in Eq. (2) [25]. In case of steel, 1 μA/cm² is equal to 9.0885 mg/cm² year as shown in results of Section 3.3.

Results of corrosion rate (CR) of steel embedded in concrete at different exposure period are shown in Fig. 14 to 17. The corrosion severity mentioned in Table 4 is also shown in these figures.

For samples under normal environment, corrosion rate slightly decreased along with an increase of exposure period in each dry or moist state, as shown from Fig. 14 to 17. This attributed to the enhancement of passive film by the progressive hydration reactions of cement that produced more alkaline species such as KOH, NaOH and $Ca(OH)_2$ [38], as well as an increase of the electrical resistivity.

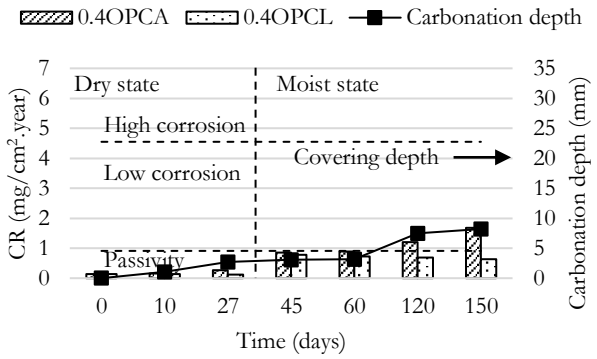

Fig. 14. Corrosion rate of steel embedded in 0.4OPC concrete in both exposures.

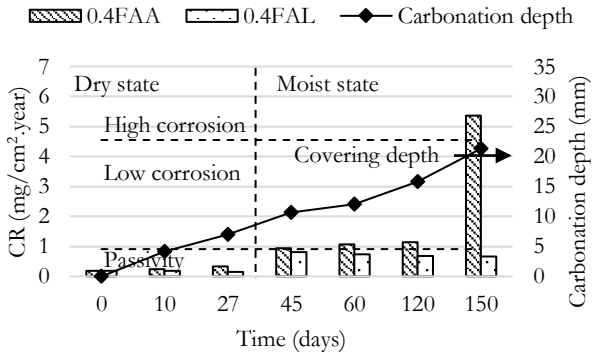

Fig. 15. Corrosion rate of steel embedded in 0.4FA concrete in both exposures.

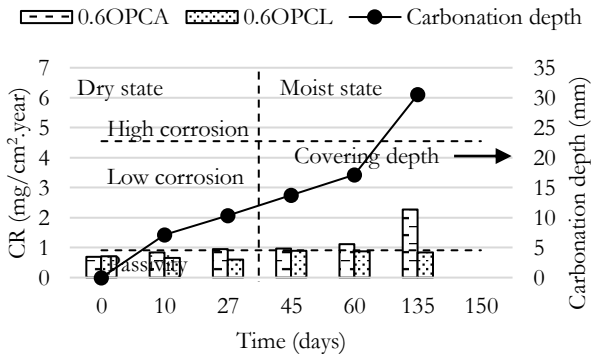

Fig. 16. Corrosion rate of steel embedded in 0.6OPC concrete in both exposures.

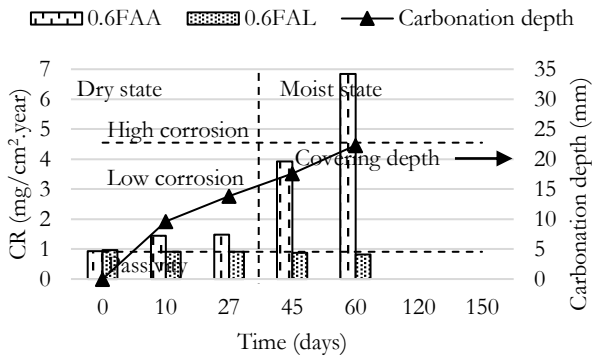

Fig. 17. Corrosion rate of steel embedded in 0.6FA concrete in both exposures.

In contrast, the corrosion rates of samples in accelerated carbonation increased with an increase of exposure period. It should be noted that even carbonation depth did not reach the steel (carbonation depth is less than covering depth), corrosion rate started to increase. This result is in a good agreement with other studies [3, 38, 39]. This attributed to the endangerment of passive film by the progression of carbonation depth.

With the same w/b ratio, the steel embedded in OPC concrete showed lower corrosion rate than that of the steel in FA concrete. This result is in good agreement with other studies [3, 40]. This is because reduction of pH in FA concrete, due to reduction of cement content as well as pozzolanic reaction, weakens the passive film even fly ash concrete has higher electrical resistivity.

Specimen with higher w/b ratio showed higher corrosion rate than that of the lower w/b specimen. This attributes to the lower pH value of high w/b concrete due to lower amount of cement content. In addition, this is because high w/b concrete has lower electrical resistivity.

For repair materials, corrosion rate are comparable to that of 0.6OPC concrete and higher than that of 0.4OPC concrete, as shown from Fig. 18 to 23. Only corrosion rate of PSKA and PSBA specimens increased over exposure period, as shown in Figures 18 and 19, respectively. This attributes to the endangerment of passive film by the progression of carbonation front in these two materials.

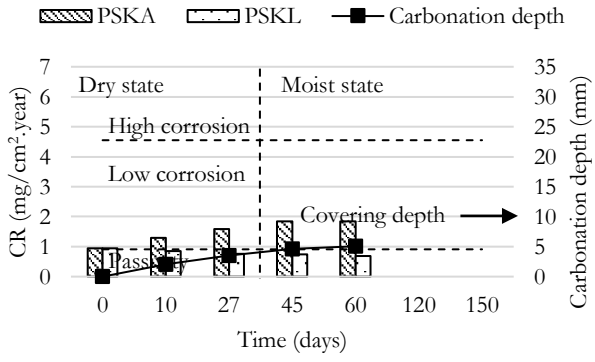

Fig. 18. Corrosion rate of steel embedded in PSK in both exposures.

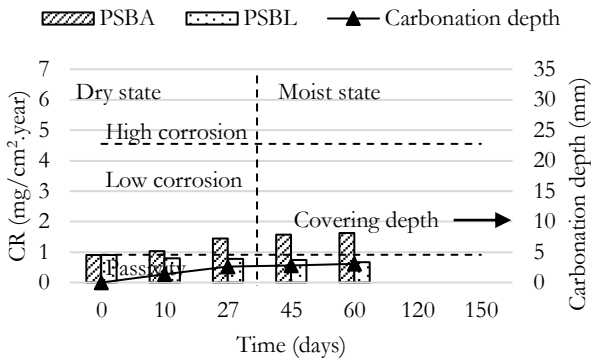

Fig. 19. Corrosion rate of steel embedded in PSB in both exposures.

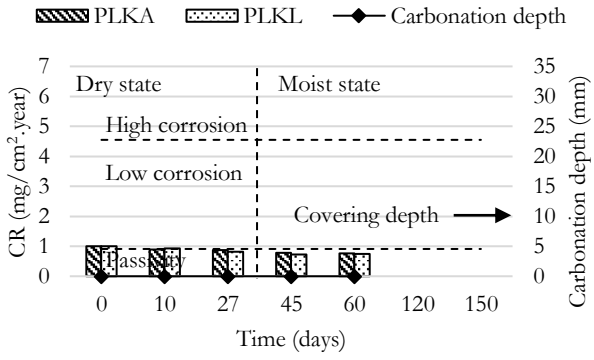

Fig. 20. CR of steel embedded in PLK in both exposures.

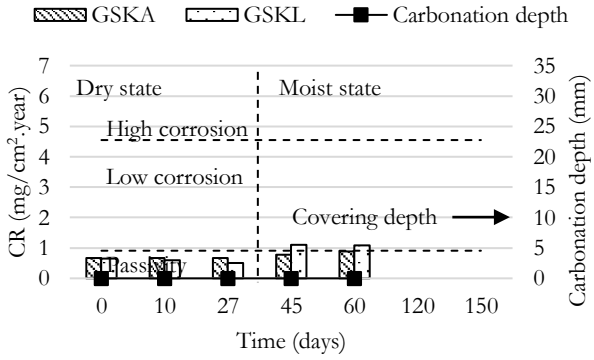

Fig. 21. CR of steel embedded in GSK in both exposures.

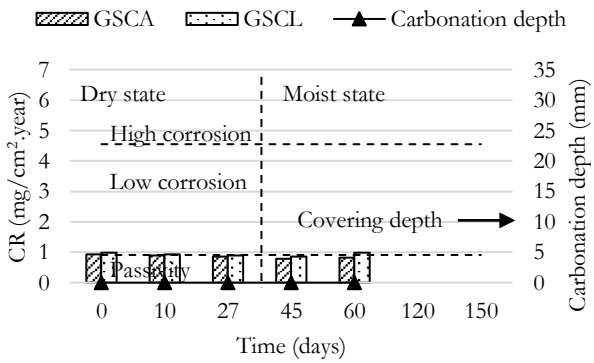

Fig. 22. CR of steel embedded in GSC in both exposures.

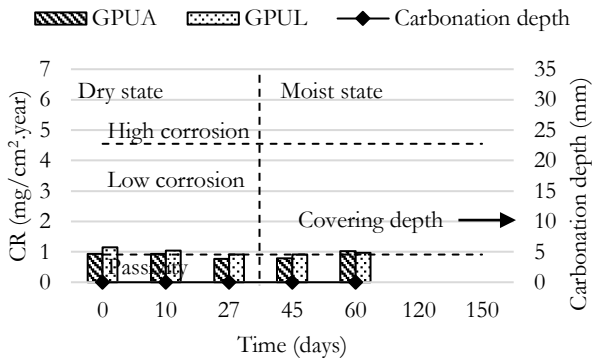

Fig. 23. CR of steel embedded in GPU in both exposures.

3.4. Guideline to evaluate carbonation-induced corrosion

The carbonation adversely affects to strength of passive film, thus corrosion rate increase. From Fig. 24, corrosion rate increased as remaining non-carbonated depth (RD) decreased. Results also show good relationship which depends on type of binder. The relationship between remaining uncarbonated depth and corrosion rate is shown in Fig. 24(a) and (b) for OPC and FA samples, respectively.

Based on time to cracking due to corrosion, corrosion severity and corrosion rate are classified as shown in Table 6 [41]. Then RD can be determined based on relationship with corrosion rate as shown in Fig. 24. So measurement of carbonation depth is not only for corrosion initiation checking but also for evaluating corrosion severity.

Guideline to evaluate corrosion due to carbonation is proposed as shown in Table 6 based on corrosion severity [41]. As shown, steel corrosion is initiated if remaining uncarbondated depth is less than 10.6 and 13 mm for OPC and FA concrete, respectively. This is due to FA concrete has lower pH and passivity can be destroyed faster.

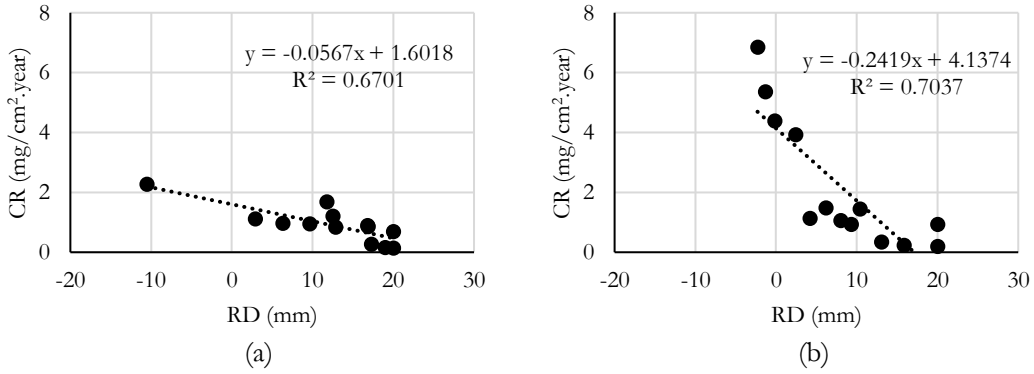

Fig. 24. Relationship between remaining uncarbonated depth (RD) and corrosion rate (CR) of: (a) steel in OPC concretes, (b) steel in FA concretes.

Table 6. Corrosion evaluation based on remaining uncarbonated depth.

Description	Time to corrosion crack (year)	Corrosion rate (mg/cm²-yr)	Remaining uncarbonated depth (mm)	
			OPC concrete	FA concrete
Passivity	>10	0 to1	>10.6	>13
Low corrosion	5 to 10	1 to 2	10.6 to -7	13 to 9
High corrosion	3 to 5	2 to 3.3	-7 to -30	9 to 3
Extremely high corrosion	< 3	> 3.3	<-30	<3

4. Conclusions

This study can be concluded as follow:

- Both of patching and grouting repair materials show higher carbonation resistance than normal concrete. There is no carbonation progress on grout-repair materials.
- The electrical resistivity of repair material is also comparable to concrete. The electrical resistivity of both concrete and repair material increased with an increase of exposure period due to hydration and carbonation.
- The corrosion rate of steel embedded in concrete and repair material increased with an increase of carbonation depth, even it does not reach the steel surface.
- The guideline to evaluate the severity of corrosion based on remaining uncarbonated depth is proposed.

Acknowledgement

The authors would like to acknowledge the National Metal and Materials Technology Center for supporting the equipment during the research and the Center of Excellence in Material Science, Construction and Maintenance Technology Project, Thammasat University. This study was supported by Chair Professor Grant (P-19-52302), the National Science and Technology Development Agency (NSTDA), Thailand.

References

[1] D. Bastidas, A. Fernández-Jiménez, A. Palomo, and J. González, "A study on the passive state stability of steel embedded in activated fly ash mortars," *Corrosion Science,* vol. 50, no. 4, pp. 1058-1065, 2008.

[2] L. Bertolini, B. Elsener, P. Pedeferri, E. Redaelli, and R. B. Polder, *Corrosion of steel in concrete: prevention, diagnosis, repair*. John Wiley & Sons, 2013.

[3] M. Serdar, S. Poyet, V. L'Hostis, and D. Bjegović, "Carbonation of low-alkalinity mortars: Influence on corrosion of steel and on mortar microstructure," *Cement and Concrete Research,* vol. 101, pp. 33-45, 2017.

[4] V. Ngala and C. Page, "Effects of carbonation on pore structure and diffusional properties of hydrated cement pastes," *Cement and concrete research,* vol. 27, no. 7, pp. 995-1007, 1997.

[5] E. A. B. Khalil and M. Anwar, "Carbonation of ternary cementitious concrete systems containing fly ash and silica fume," *Water Science,* vol. 29, no. 1, pp. 36-44, 2015.

[6] B. Dong *et al.*, "Characterization of carbonation behavior of fly ash blended cement materials by the electrochemical impedance spectroscopy method," *Cement and Concrete Composites,* vol. 65, pp. 118-127, 2016.

[7] P. H. Borges, J. O. Costa, N. B. Milestone, C. J. Lynsdale, and R. E. Streatfield, "Carbonation of CH and C–S–H in composite cement pastes containing high amounts of BFS," *Cement and Concrete Research,* vol. 40, no. 2, pp. 284-292, 2010.

[8] Z. Shi *et al.*, "Experimental studies and thermodynamic modeling of the carbonation of Portland cement, metakaolin and limestone mortars," *Cement and Concrete Research,* vol. 88, pp. 60-72, 2016.

[9] J. Khunthongkeaw, S. Tangtermsirikul, and T. Leelawat, "A study on carbonation depth prediction for fly ash concrete," *Construction and building materials,* vol. 20, no. 9, pp. 744-753, 2006.

[10] K. Sisomphon and L. Franke, "Carbonation rates of concretes containing high volume of pozzolanic materials," *Cement and Concrete Research,* vol. 37, no. 12, pp. 1647-1653, 2007.

[11] B. Salvoldi, H. Beushausen, and M. Alexander, "Oxygen permeability of concrete and its relation to carbonation," *Construction and Building Materials,* vol. 85, pp. 30-37, 2015.

[12] A. Morandeau, M. Thiéry, and P. Dangla, "Impact of accelerated carbonation on OPC cement paste blended with fly ash," *Cement and Concrete Research,* vol. 67, pp. 226-236, 2015.

[13] V. G. Papadakis, "Effect of supplementary cementing materials on concrete resistance against carbonation and chloride ingress," *Cement and concrete research,* vol. 30, no. 2, pp. 291-299, 2000.

[14] M. Auroy *et al.*, "Impact of carbonation on unsaturated water transport properties of cement-based materials," *Cement and concrete research,* vol. 74, pp. 44-58, 2015.

[15] M. M. Al-Zahrani, M. Maslehuddin, S. U. Al-Dulaijan, and M. Ibrahim, "Mechanical properties and durability characteristics of polymer- and cement-based repair materials," *Cement and Concrete Composites,* vol. 25, no. 4, pp. 527-537, 2003.

[16] G. Glass, C. Page, and N. Short, "Factors affecting the corrosion rate of steel in carbonated mortars," *Corrosion Science,* vol. 32, no. 12, pp. 1283-1294, 1991.

[17] L. Parrott, "A study of carbonation-induced corrosion," *Magazine of Concrete Research,* vol. 46, no. 166, pp. 23-28, 1994.

[18] E. Chávez-Ulloa, R. Camacho-Chab, M. Sosa-Baz, P. Castro-Borges, and T. Pérez-López, "Corrosion process of reinforced concrete by carbonation in a natural environment and an accelerated test chamber," *Int. J. Electrochem. Sci,* vol. 8, no. 7, pp. 9015-9029, 2013.

[19] ASTM, "ASTM C150/C150M-12: Standard specification for Portland cement," ASTM International West Conshohocken, PA, USA, 2012.

[20] T. I. Standards, "TIS 2135: Standard specification for coal fly ash for using as an admixture in concrete," Ministry of Industry, Thailand, 2002.

[21] K. Gowers and S. Millard, "Measurement of concrete resistivity for assessment of corrosion," *ACI Materials Journal,* vol. 96, no. 5, 1999.

[22] ASTM C642, "Standard test method for density, absorption, and voids in hardened concrete," *C642–13,* 2013.

[23] M. Stern and A. L. Geary, "Electrochemical polarization I. A theoretical analysis of the shape of polarization curves," *Journal of the electrochemical society,* vol. 104, no. 1, pp. 56-63, 1957.

[24] D. M. Bastidas, J. González, S. Feliu, A. Cobo, and J. Miranda, "A quantitative study of concrete-embedded steel corrosion using potentiostatic pulses," *Corrosion,* vol. 63, no. 12, pp. 1094-1100, 2007.

[25] ASTM, "ASTM G102-89(2015)e1, Standard Practice for Calculation of Corrosion Rates and Related Information from Electrochemical Measurements," *ASTM International,* vol. 89, pp. 1-7, 2015.

[26] D. Network, "Manual de inspección, evaluación y diagnóstico de corrosión en estructuras de hormigón armado," *CYTED Programe,* 1997.

[27] J. M. Chi, R. Huang, and C. Yang, "Effects of carbonation on mechanical properties and durability of concrete using accelerated testing method,"

Journal of Marine Science and Technology, vol. 10, no. 1, pp. 14-20, 2002.

[28] E. I. Moreno, E. Cob-Sarabia, and P. C. Borges, "Corrosion rates from carbonated concrete specimens," in *CORROSION 2004*, 2004: NACE International.

[29] R. A. Medeiros-Junior and M. G. Lima, "Electrical resistivity of unsaturated concrete using different types of cement," *Construction and Building Materials,* vol. 107, pp. 11-16, 2016.

[30] C. Andrade and R. D'andrea, "The electrical resistivity as a control parameter of the concrete and its durability (In Spanish: La resistividad eléctrica como parámetro de control del hormigón y de su durabilidad)," *Revista ALCONPAT,* vol. 1, no. 2, pp. 90-98, 2011.

[31] F. Presuel-Moreno, Y. Y. Wu, and Y. Liu, "Effect of curing regime on concrete resistivity and aging factor over time," *Construction and Building Materials,* vol. 48, pp. 874-882, 2013.

[32] F. Deschner *et al.*, "Hydration of Portland cement with high replacement by siliceous fly ash," *Cement and Concrete Research,* vol. 42, no. 10, pp. 1389-1400, 2012.

[33] P. Mehta and O. Gjørv, "Properties of portland cement concrete containing fly ash and condensed silica-fume," *Cement and Concrete Research,* vol. 12, no. 5, pp. 587-595, 1982.

[34] S. W. Hnin, P. Sancharoen, and S. Tangtermsirikul, "Effects of Concrete Mix Proportion on Electrical Resistivity of Concrete," *Materials Science Forum,* vol. 866, pp. 68-72, 2016.

[35] I. O. Yaman, N. Hearn, and H. M. Aktan, "Active and non-active porosity in concrete Part I: Experimental evidence," *Materials and Structures,* vol. 35, no. 2, p. 102, 2002/03/01 2002.

[36] M. G. Hernández, M. A. G. Izquierdo, A. Ibáñez, J. J. Anaya, and L. G. Ullate, "Porosity estimation of concrete by ultrasonic NDE," *Ultrasonics,* vol. 38, no. 1, pp. 531-533, 2000.

[37] S. W. Hnin, "Factors Affect Concrete Electrical Resistivity And Its Modelling," MSc., Civil Engineering And Technology, Thammasat University, 2017.

[38] W. Aperador, R. Mejía de Gutiérrez, and D. M. Bastidas, "Steel corrosion behaviour in carbonated alkali-activated slag concrete," *Corrosion Science,* vol. 51, no. 9, pp. 2027-2033, 2009.

[39] C. Andrade and R. Buják, :Effects of some mineral additions to Portland cement on reinforcement corrosion," *Cement and Concrete Research,* vol. 53, pp. 59-67, 2013.

[40] M. P. Kulakowski, F. M. Pereira, and D. C. C. D. Molin, "Carbonation-induced reinforcement corrosion in silica fume concrete," *Construction and Building Materials,* vol. 23, no. 3, pp. 1189-1195, 2009.

[41] T. V. P. Dong, "Modeling of electrochemical corrosion of reinforcing steel in patching-repaired reinforced concrete," Doctoral Dissertation, School of Civil Engineering and Technolgoy, Thammasat University, Thailand, 2019.

Sothyrak Rath, photograph and biography not available at the time of publication.

Pakawat Sancharoen, photograph and biography not available at the time of publication.

Pitichon Klomjit, photograph and biography not available at the time of publication.

Somnuk Tangtermsirikul, photograph and biography not available at the time of publication.